Extension of Tlusty's law for the identification of chatter stability lobes in multi-dimensional cutting processes

Andreas Otto[a,*], Stefan Rauh[b,c], Martin Kolouch[b], Günter Radons[a]

[a] *Institute of Physics, Chemnitz University of Technology, 09107 Chemnitz, Germany*
[b] *Institute for Machine Tools and Production Processes, Chemnitz University of Technology, 09107 Chemnitz, Germany*
[c] *Fraunhofer Institute for Machine Tools and Forming Technology IWU, Reichenhainer Straße 88, 09126 Chemnitz, Germany*

Abstract

Chatter vibrations in cutting processes are studied in the present paper. A unified approach for the calculation of the stability lobes for turning, boring, drilling and milling processes in the frequency domain is presented. The method can be used for a fast and reliable identification of the stability lobes and can take into account nonlinear shearing forces, as well as process damping forces. The applicability of Tlusty's law, which is a simple scalar relationship between the real part of the oriented transfer function of the structure and the limiting chip width, is extended to milling and any other multi-dimensional chatter problem without neglecting the coupled dynamics. The given analysis is suitable for getting a deep understanding of the chatter stability dependent on the parameters of the cutting process and the structure. Basic examples based on experimental data of real machine tools include the dependence of the stability behavior on the rotational direction in turning, the effect of axial-torsional structural coupling in drilling, and the dynamics of slot milling.

Keywords:
chatter, vibration, stability, turning, milling, drilling, boring

1. Introduction

The efficiency of machining operations is sometimes limited by the occurrence of undesired chatter vibrations. Chatter leads to noise, bad surface finish and increased wear of tools and machine tool components. For increasing productivity and quality the dynamic simulation of mechanical interactions between the machine tool and the cutting process is important. In particular, the prediction of the so-called stability lobes of chatter is used for optimizing the cutting process. Since more than 50 years [1, 2] it is known that the regenerative mechanism is mainly responsible for undesired chatter vibrations in cutting processes. The wavy outer surface of the chip due to vibrations at the previous cut generates dynamic variations of the cutting force, which again creates new waves on the inner surface of the chip. Altintas and Weck [3] and Altintas [4] give a good overview on the stability lobe theory of different metal cutting and grinding processes.

Current research in the field of chatter stability is dedicated to the influence of process damping [5, 6, 7, 8], the effect of the nonlinear cutting force behavior [9], and the influence of non-constant [10, 11, 12, 13] and non-uniform delays [15, 16, 17] on the stability behavior of cutting processes. The

*Corresponding author
Tel.: +49 (371) 531 37717
Fax.: +49 (371) 531 837717
E-Mail: andreas.otto@physik.tu-chemnitz.de

aforementioned literature presents good methods and results for the prediction of stability lobes for various cutting processes and geometries. Nevertheless, already for very simple cutting process models it is sometimes difficult to understand the dependence of the chatter stability on the structural dynamics and the process parameters. A good understanding of the chatter mechanism can contribute to an optimization of the productivity already in the design stage of machine tools [18, 19]. Furthermore, knowing some simple relationships between structural behavior, cutting conditions and chatter stability helps to find optimal process parameters and to fix problems with undesired vibrations during manufacturing.

In this paper a unified model for the dynamic cutting force in machining is established in Sec. 2. The model is kept as simple as possible, since the present paper is focused on a deeper understanding of the regenerative chatter mechanism. In Sec. 3 the chatter stability analysis of cutting processes is put into an universal theoretical framework in the frequency domain. The presented analysis can be used for a fast calculation of the stability lobes for turning, boring, milling and drilling processes with various process geometries and machine tools. It is based on the theory of Altintas and Budak [20] for milling, but the procedure for solving the eigenvalue problem is different from the existing literature [3, 4, 6, 20, 21, 22]. As a consequence new insights into the dynamics of chatter vibrations are available. Examples for the dynamics of turning, drilling and milling based on experimental data of real machine tools are shown in Sec. 4. In particular the dependence of the stability lobes on the rotational direction of the spindle in turning and the effect of structural coupling for torsional-axial chatter of twist drills is explained. Furthermore an accurate scalar approximation for the stability analysis of slot milling is derived.

2. Dynamic cutting force model

For simplicity the basic model is established for a static process geometry with only one cutting tooth and a linear cutting force model. The geometry of a turning process as an example of such processes is shown in Fig. 1. The unit vector $\mathbf{e}_h$ defines the

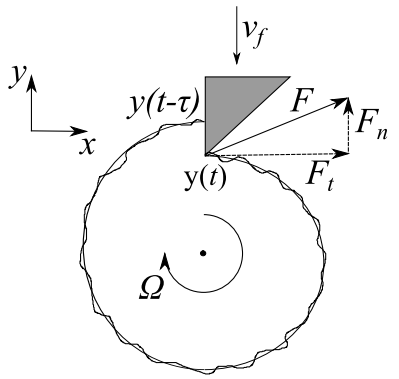

Figure 1: Geometry of a turning process for clockwise spindle rotation. The symbols are explained in the text.

direction normal to the nominal cut surface, which is equal to the radial direction at the tool tip in the example of Fig. 1. With this definition of $\mathbf{e}_h$, the chip thickness $h(t)$ at time t can be written as

$$h(t) = h_0 + \mathbf{e}_h^T(\mathbf{r}(t-\tau) - \mathbf{r}(t)), \qquad (1)$$

where ^{T} denotes transposition. In Eq. (1) h_0 is the static chip thickness due to the constant feed velocity v_f and τ is the time delay between two subsequent cuts. The vector $\mathbf{r}(t)$ specifies dynamical displacements from a reference position of the tool tip, generated by the cutting force at time t. The displacement vector $\mathbf{r}$ is specified in a fixed machine tool coordinate system. In general, it contains two lateral displacements x and y, axial displacements z and torsional displacements θ around the spindle axis.

The cutting force $\mathbf{F}_{tn} = (F_t, F_n)^T$ is specified in tangential F_t and normal F_n forces at the cutting edge (see Fig. 1) and contains shearing forces proportional to the chip thickness $h(t)$, as well as process damping forces assumed to be proportional to the velocity $\dot{\mathbf{r}}(t)$ of the vibration

$$\mathbf{F}_{tn}(t) = bK_{tc}\left[\begin{pmatrix}1\\ k_{nc}\end{pmatrix} h(t) - \begin{pmatrix}k_{td}\\ k_{nd}\end{pmatrix} \mathbf{e}_h^T \tau \dot{\mathbf{r}}(t)\right]. \qquad (2)$$

Here, b is the chip width and K_{tc} is the cutting pressure of the shearing force in tangential direction. The dimensionless coefficients k_{nc}, k_{td} and k_{nd} are the ratios of the cutting pressure of the normal shearing

force k_{nc}, as well as the cutting pressure of the tangential k_{td} and normal k_{nd} process damping force to K_{tc}. According to [5, 8, 21] the damping force coefficients can be determined by

$$\begin{pmatrix} k_{td} \\ k_{nd} \end{pmatrix} = \begin{pmatrix} \mu \\ 1 \end{pmatrix} \frac{C}{K_{tc} R\delta}, \quad R\delta = V\tau, \tag{3}$$

with the process damping coefficient C, the cutting velocity V, tool or workpiece radius R and the coefficient of friction μ. The angle δ (in rad) is the angle of rotation of the spindle between two successive cuts at the same workpiece position. For the turning example of Fig. 1, $\delta = 2\pi$, and for milling and drilling processes, δ is equal to the angle beetween the cutting teeth of the tool.

For the chatter stability analysis only the dynamic part of the cutting force without the static force due to the static chip thickness h_0 is relevant. The dynamic load vector $\mathbf{F} = (F_x, F_y, F_z, M)^T$ is presented in fixed machine tool coordinates to avoid the necessity of a modal analysis of the structure. It can be described by

$$\mathbf{F}(t) = bK_{tc} \left[\mathbf{B}_c (\mathbf{r}(t-\tau) - \mathbf{r}(t)) - \mathbf{B}_d \tau \dot{\mathbf{r}}(t) \right]. \tag{4}$$

In general the 4×4 coefficient matrices $\mathbf{B}_c$ and $\mathbf{B}_d$ are specified by

$$\mathbf{B}_c = \mathbf{T} \begin{pmatrix} 1 \\ k_{nc} \end{pmatrix} \mathbf{e}_h^T, \quad \mathbf{B}_d = \mathbf{T} \begin{pmatrix} k_{td} \\ k_{nd} \end{pmatrix} \mathbf{e}_h^T. \tag{5}$$

The matrix $\mathbf{T}$ is a 4×2 dimensional matrix, which transforms the two dimensional cutting force vector $\mathbf{F}_{tn}$ of Eq. (2) at the cutting edge into the four dimensional load vector $\mathbf{F}$ of Eq. (4). The tangential and normal direction at the cutting edge can vary with respect to the fixed machine tool coordinate system. In this case or for tools with multiple teeth or a nonlinear cutting force behavior we refer to Appendix A for the calculation of the matrices $\mathbf{B}_c$ and $\mathbf{B}_d$.

The entries $\{\mathbf{B}_c\}_{kl}$ and $\{\mathbf{B}_d\}_{kl}$ of the coefficient matrices are typically called directional factors. The multiplication of the directional factors with the scalar constants b and K_{tc} specifies variations of the kth component of the load vector $\mathbf{F}$ due to a variation of the lth component of the displacement vector $\mathbf{r}$. Note that the same approach can be followed in modal coordinates of the machine tool structure. In this case the vector $\mathbf{r}$ contains the modal displacements of M number of modes, the M-dimensional vector $\mathbf{e}_h^T$ projects modal displacements into chip thickness variations and the $M \times 2$ dimensional matrix $\mathbf{T}$ projects tangential and normal cutting forces into the load on each mode. In a modal description the directional factors $\{\mathbf{B}_c\}_{kl}$ and $\{\mathbf{B}_d\}_{kl}$ times bK_{tc} specify variations of the load on the kth mode due to structural displacements of the lth mode, with $k, l = 1 \dots M$.

3. Frequency domain stability analysis

3.1. Efficient approach for the identification of stability lobes

The stability lobes are lobed curves in the parameter plane spanned by spindle speed $\Omega = \delta/\tau$ and chip width b. They separate stable and unstable parameter regions. Directly on the stability lobes the process is marginally stable and the structure vibrates with chatter frequency ω_c and constant amplitudes. Hence, a calculation of the stability lobes in the frequency domain is useful. With the frequency response functions (FRFs) $\Phi_{kl}(\omega)$, $k, l \in \{x, y, z, \theta\}$, the dynamic displacements of the structure can be described by

$$\hat{\mathbf{r}}(\omega) = \mathbf{\Phi}(\omega) \hat{\mathbf{F}}(\omega), \tag{6a}$$

$$\begin{pmatrix} \hat{x} \\ \hat{y} \\ \hat{z} \\ \hat{\theta} \end{pmatrix} = \begin{pmatrix} \Phi_{xx} & \Phi_{xy} & \Phi_{xz} & \Phi_{x\theta} \\ \Phi_{yx} & \Phi_{yy} & \Phi_{yz} & \Phi_{y\theta} \\ \Phi_{zx} & \Phi_{zy} & \Phi_{zz} & \Phi_{z\theta} \\ \Phi_{\theta x} & \Phi_{\theta y} & \Phi_{\theta z} & \Phi_{\theta\theta} \end{pmatrix} \begin{pmatrix} \hat{F}_x \\ \hat{F}_y \\ \hat{F}_z \\ \hat{M} \end{pmatrix}, \tag{6b}$$

where $\hat{\mathbf{u}}(\omega)$ denotes the Fourier transformation of some vector $\mathbf{u}(t)$,

$$\hat{\mathbf{u}}(\omega) = \frac{1}{\sqrt{2\pi}} \int_{-\infty}^{\infty} \mathbf{u}(t)\, \mathrm{e}^{-i\omega t}\, dt. \tag{7}$$

By putting the cutting force of Eq. (4) in its frequency domain representation into Eq. (6a), a closed loop for

regenerative chatter vibrations at the stability lobes is obtained

$$\hat{\mathbf{r}}(\omega) = bK_{tc}\mathbf{\Phi}(\omega)\left[\mathbf{B}_c(\mathrm{e}^{-i\omega\tau}-1) - \mathbf{B}_d i\omega\tau\right]\hat{\mathbf{r}}(\omega). \tag{8}$$

Eq. (8) is only valid for constant coefficient matrices $\mathbf{B}_c$ and $\mathbf{B}_d$ and constant spindle speeds Ω. If the coefficient matrices are time-variant a zeroth-order approximation (see Appendix A) gives in most cases accurate results for the stability lobes. Deviations may occur for milling with low radial immersion and a small number of teeth [4] or for unequal tooth pitch [7]. In these cases and in the case of spindle speed variation a multifrequency approach [4, 10, 17] is necessary, which is not discussed here.

Eq. (8) has the form of an eigenvalue equation, where the eigenvalues λ can be defined as

$$\lambda\mathbf{u} = \mathbf{\Phi}(\omega)\left[\mathbf{B}_c(\mathrm{e}^{-i\omega\tau}-1) - \mathbf{B}_d i\omega\tau\right]\mathbf{u}. \tag{9}$$

The eigenvalues $\lambda = \lambda(\omega,\tau) = \lambda_r(\omega,\tau) + i\lambda_i(\omega,\tau)$ and the eigenvectors $\mathbf{u} = \mathbf{u}(\omega,\tau)$ of Eq. (9) depend on the frequency ω and the delay τ. In the direction of the eigenvectors $\mathbf{u}(\omega,\tau)$ Eq. (8) simplifies to the scalar relationship $1 = K_{tc}b\lambda(\omega,\tau)$. Because chip width b and cutting pressure K_{tc} are real-valued, the imaginary parts λ_i of the eigenvalues for ω corresponding to the chatter frequency must vanish

$$\lambda_i(\omega_c,\tau) = 0. \tag{10}$$

The stability lobes can be calculated from the real part λ_r of the maximal eigenvalue with vanishing imaginary part as

$$b_c = \frac{1}{K_{tc}\lambda_r(\omega_c,\tau)}. \tag{11}$$

Eq. (11) and Eq. (10) specify the relationship between chatter frequencies ω_c, critical chip widths b_c and delays τ, where purely periodic vibrations at the tool tip with $\mathbf{r}(t) \propto \mathbf{u}(\omega_c,\tau)\,\mathrm{e}^{i\omega_c t}$ are possible. For vanishing chip widths $b \to 0$ vibrations at the tool tip decay exponentially because of structural damping and consequently the system is stable. For increasing chip width b and fixed delay τ the stability behavior changes exactly at the lowest critical chip width b_c, where a periodic structural vibration is possible. Thus, according to Eq. (11) only the largest real part λ_r of the eigenvalues $\lambda(\omega_c,\tau)$ is relevant for the calculation of the stability lobes. The following procedure is proposed.

1. Determine the nonzero eigenvalues $\lambda(\omega,\tau)$ of Eq. (9) analytically as a function of ω and τ.
2. Select a spindle speed Ω or a time delay τ.
3. Calculate the possible chatter frequencies ω_c for given τ by Eq. (10).
4. The stability limit b_c is specified by the largest λ_r of all pairs ω_c, τ according to Eq. (11).

In higher dimensional problems it can be useful to perform step two before step one and calculate the eigenvalues of Eq. (9) for the selected delays τ and a frequency sample numerically.

3.2. Application of Tlusty's law to multi-dimensional cutting processes

If the influence of process damping can be neglected, $\mathbf{B}_d = \mathbf{0}$, the eigenvalues of Eq. (9) can be written as follows

$$\lambda(\omega,\tau) = \sigma(\omega)(\mathrm{e}^{-i\omega\tau}-1), \tag{12a}$$

$$\text{with} \quad \sigma(\omega)\mathbf{v}(\omega) = \mathbf{\Phi}(\omega)\mathbf{B}_c\mathbf{v}(\omega). \tag{12b}$$

Here, the eigenvalues $\sigma(\omega) = \sigma_r(\omega) + i\sigma_i(\omega)$ and the eigenvectors $\mathbf{v} = \mathbf{v}(\omega)$ depend only on the frequency ω. If Eq. (10) is applied to Eq. (12a), the relation $\lambda_r(\omega_c,\tau) = -2\sigma_r(\omega_c)$ between the real parts of λ and σ holds for all delays τ. Putting this relation into Eq. (11) reveals

$$b_c = -\frac{1}{2K_{tc}\sigma_r(\omega_c)}. \tag{13}$$

Eq. (13) is a generalization of the stability law of Tlusty [1, 3, 8] to multi-dimensional cutting processes. It can be used to calculate the stability border for a given chatter frequency ω_c. The time delay τ corresponding to the chatter frequency ω_c can be determined by substituting Eq. (12a) with $\omega = \omega_c$ into Eq. (10) and solving for τ. The generalized oriented transfer functions $\sigma(\omega)$ are all non-vanishing eigenvalues of Eq. (12b). Only chatter frequencies ω_c, with $\sigma_r(\omega_c) < 0$ for at least one of the generalized oriented

transfer functions $\sigma(\omega_c)$, can appear at the stability lobes. The negative minimum of the real part $\sigma_r(\omega_c)$ of all oriented transfer functions specifies the minimum of the limiting depth of cut b_c. The eigenvectors $\mathbf{v}$ corresponding to the eigenvalues σ characterize the shape of the critical chatter vibrations at the stability border with $\mathbf{r}(t) \propto \mathbf{v}(\omega_c)\, \mathrm{e}^{i\omega_c t}$.

Eq. (13) is frequently used for one-dimensional stability problems as for example for turning processes. One-dimensional stability problems are either characterized by structures, which are flexible only in one direction $\mathbf{e}_v$ and rigid in the other directions, or by only one fixed normal direction $\mathbf{e}_v = \mathbf{e}_h$, as for example the y-direction in the turning process of Fig. (1). In this case, there is only a single nonzero eigenvalue of Eq. (12b), which is called oriented transfer function and can be specified by

$$\sigma(\omega) = \mathbf{e}_v^T \mathbf{\Phi}(\omega) \mathbf{B}_c \mathbf{e}_v, \tag{14}$$

where the unit vector $\mathbf{e}_v$ defines the relevant direction for the regenerative effect. Eq. (14) is a superposition of the FRFs Φ_{kl} at the tool tip with $k, l \in \{x, y, z, \theta\}$. Concrete examples for oriented transfer functions similar to Eq. (14) can be found in [3].

In multi-dimensional stability problems, as for example for typical milling processes, the coupled two-dimensional dynamics is relevant for the regenerative effect. For milling several attempts have been made to establish an oriented transfer function in the form of a superposition of the FRFs of the structure to use Eq. (13) for the stability analysis. Some of them are summarized in [3]. However, due to their structural similarity to Eq. (14) these approaches for the oriented transfer function are only one-dimensional approximations of the process. They only give accurate results for special cases, as for example, if the structural behavior at the tool tip is dominated by vibrations only in one direction. With our definition for the generalized oriented transfer functions $\sigma(\omega)$ as eigenvalues of the matrix $\mathbf{\Phi}(\omega)\mathbf{B}_c$, the applicability of Eq. (13) is extended to an exact stability analysis of multi-dimensional cutting processes.

3.3. Discussion of the present approach

In the absence of process damping, $\mathbf{B}_d = 0$, the identification of stability lobes based on the analysis of the eigenvalues of the closed loop for regenerative chatter similar to Eq. (8) for multi-dimensional cutting processes can be already found in the literature. In [3, 4, 6, 20] a solution for the two dimensional coupled dynamics in milling and in [22] a solution for the coupled dynamics in drilling is presented. In these papers the eigenvalues $\Lambda(\omega) = \Lambda_r(\omega) + i\Lambda_i(\omega)$ are used for the stability analysis, corresponding to the eigenvalue problem

$$\mathbf{v}_F(\omega) = c_1 \Lambda(\omega) \mathbf{B}_c \mathbf{\Phi}(\omega) \mathbf{v}_F(\omega), \tag{15}$$

where c_1 is some process-specific dimensionless constant. The limiting chip width b_c can be calculated from the eigenvalues Λ by [3, 4, 6, 20, 22]

$$b_c = -\frac{c_1 \Lambda_r(\omega_c)}{2K_{tc}} \left(1 + \frac{\Lambda_i^2(\omega_c)}{\Lambda_r^2(\omega_c)}\right). \tag{16}$$

Here, the eigenvectors $\mathbf{v}_F$ of Eq. (15) characterize the shape of the critical force vibrations at the stability border with $\mathbf{F}(t) \propto \mathbf{v}_F(\omega_c)\, \mathrm{e}^{i\omega_c t}$. Eq. (15) and Eq. (16) are equivalent to Eq. (12b) and Eq. (13), respectively, where the relationships between the eigenvectors and eigenvalues are given by

$$\mathbf{v}(\omega) = \mathbf{\Phi}(\omega) \mathbf{v}_F(\omega), \tag{17a}$$

$$\sigma(\omega) = \frac{1}{c_1 \Lambda(\omega)}. \tag{17b}$$

Eq. (13) or Eq. (16) can be used for the optimization of the structural behavior of the machine tool [18, 19] by a modification of the eigenvalues $\sigma(\omega)$ or $\Lambda(\omega)$. The advantages of our generalization of Tlusty's law, presented in Sec. 3.2, are the simple relationship Eq. (13) between σ and b_c, and the interpretation of σ as generalized oriented transfer functions. An increase of the negative minimum of the real part σ_r of the generalized oriented transfer functions leads to a stabilization of the process. If, instead, the eigenvalues Λ of Eq. (15) are used, a more complex expression of the eigenvalues Λ has to be optimized, as can be seen from Eq. (16). In addition,

for some multi-dimensional problems very simple relationships between the real part $\sigma_r(\omega)$ and the FRFs $\Phi_{kl}(\omega)$ of the structure can be derived, as can be seen for the slot milling example in Sec. 4.4

In case of process damping, $\mathbf{B}_d \neq 0$, Eq. (13) or Eq. (16) can be only used in an iterative way for the identification of the stability lobes, as proposed for example in [6, 8]. In these papers b_c is calculated with Eq. (16) without process damping and the result is used to add some additional process damping term to the structural damping. Then b_c is again calculated by Eq. (16) with the modified damping term and the procedure is repeated until the results converge. With the approach of Sec. 3.1 for the identification of the stability lobes with the eigenvalues λ as defined in Eq. (9) no iterative procedure is necessary. The stability lobes can be calculated directly with Eq. (10) and Eq. (11), as it is shown in the example in Sec. 4.1.

Furthermore, with the eigenvalues λ, the limiting chip width b_c can be calculated very efficiently for a specific spindle speed Ω, which makes it suitable for an implementation on the numerical control of a machine tool. With Eq. (13) or Eq. (16) only a relation between the limiting chip width b_c and the chatter frequency ω_c is given, whereas the corresponding spindle speed Ω has to be determined additionally. Thus, the method, presented in Sec. 3.1, for the calculation of the limiting chip width b_c can be convenient even in the case without process damping.

4. Examples

4.1. Turning with process damping

As a first example the stability of a turning process with process damping is investigated. The parameters are chosen from the example of [5, 8]. Only one structural mode in normal direction with mass $m = 0.561$ kg, damping coefficient $c = 145$ Ns/m and stiffness $k = 6.48 \times 10^6$ N/m is assumed

$$\Phi_{yy}(\omega) = \left(-m\omega^2 + i\omega c + k\right)^{-1}. \tag{18}$$

The other FRFs are assumed to be zero, i.e. the structure is assumed to be infinitely stiff in the other directions.

The geometric properties of the process are given by

$$\mathbf{e}_h = \begin{pmatrix} 0 \\ 1 \end{pmatrix}, \quad \mathbf{T} = \begin{pmatrix} \pm 1 & 0 \\ 0 & 1 \end{pmatrix}. \tag{19}$$

Depending on the rotational direction of the spindle the tangential cutting force on the tool acts in positive or negative x-direction. The geometry of the process is illustrated in Fig. 1 for the case of clockwise spindle rotation with the positive sign in the matrix $\mathbf{T}$ in Eq. (19). The axial and torsional components are dropped, because the influence of vibrations in these directions on the chip thickness is typically negligible [14]. The coefficient matrices are

$$\mathbf{B}_c = \begin{pmatrix} 0 & \pm 1 \\ 0 & k_{nc} \end{pmatrix}, \quad \mathbf{B}_d = \begin{pmatrix} 0 & \pm k_{td} \\ 0 & k_{nd} \end{pmatrix}. \tag{20}$$

Since the machine tool structure is assumed to be rigid in x-direction the eigenvalue of Eq. (9) for this example is

$$\lambda(\omega, \tau) = \Phi_{yy}(\omega)\left(k_{nc}(\mathrm{e}^{-i\omega\tau} - 1) - k_{nd} i\omega\tau\right). \tag{21}$$

It is independent of the behavior of the tangential cutting force and the rotational direction of the spindle. The eigenvector corresponding to λ in Eq. (21) is $\mathbf{u} = (0, 1)^T$. This means that the tool vibrates only in the y-direction, which is clear, because the structure is assumed to be rigid in the other directions.

The stability limits were calculated for one thousand spindle speeds with the method presented in Sec. 3.1. It takes only a few seconds on a conventional CPU, because in contrast to the method proposed in [8] no iterative procedure is necessary for the calculation of the stability lobes. The cutting force parameters $K_{tc} = 2580$ N/mm^2, $k_{nc} = 0.536$ and $k_{nd} = 0.00215$ in this example are taken from [5, 8]. The stability lobes are shown in Fig. 2 and coincide very well with the results from the literature.

4.2. Influence of rotational direction in turning

In this section a complex structural model for the turning process is considered, were no structural FRF in the x-y-plane can be neglected. Now, process damping is assumed to be negligible, $\mathbf{B}_d = \mathbf{0}$, to focus on the influence of the rotational direction on the

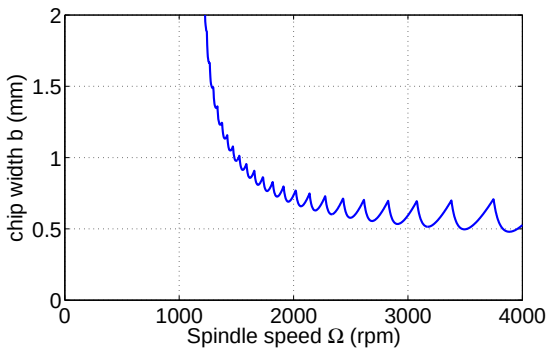

Figure 2: Stability lobes for turning with process damping calculated with the method presented in Sec. 3 and paramters as used in [8] coincide well with the results from the literature.

stability lobes. With the geometry of the previous example (see Fig. 1) and the coefficient matrix $\mathbf{B}_c$ of Eq. (20) the nonzero eigenvalue of Eq. (12b) is

$$\sigma(\omega) = \Phi_{yy}(\omega)k_{nc} \pm \Phi_{yx}(\omega). \tag{22}$$

The eigenvector corresponding to the oriented transfer function in Eq. (22) is $\mathbf{v}(\omega) = (\Phi_{xy}(\omega)k_{nc} \pm \Phi_{xx}(\omega), \Phi_{yy}(\omega)k_{nc} \pm \Phi_{yx}(\omega))^T$, which means that the shape of the tool vibration depends on the chatter frequency ω and is in general not restricted to the normal direction $\mathbf{e}_h$ as in the previous example. In contrast to Eq. (21) for a rigid structure in x-direction, the oriented transfer function σ in general depends on the rotational direction of the spindle. The positive sign of the cross FRF Φ_{yx} in Eq. (22) corresponds to clockwise spindle rotation as in Fig. 1, whereas a negative sign is associated to counterclockwise rotation of the spindle. Of course, in addition another turning tool is necessary for the same process with the inverse rotational direction, which can cause modifications of the structural FRFs Φ_{yy} and Φ_{yx}. However, due to the low mass of the turning tool compared to the mass of the machine tool, these modifications will be relevant only for tool modes at high frequencies, whereas the low frequency machine tool modes will remain almost unchanged.

The effect of the rotational direction of the spindle on the chatter instability in a real turning process is illustrated in Fig. 3. The two relevant FRF at the tool tip of a CNC lathe Gildemeister CTX 400 E, obtained by impact hammer tests, are shown in Fig. 3(a). The magnitude of the cross FRF Φ_{yx} is lower than the magnitude of the direct FRF Φ_{yy}. However, the parameter k_{nc} in the oriented transfer function σ of Eq. (22) is typically much lower than one and weakens the influence of the direct FRF on the chatter stability in relation to the influence of Φ_{yx}. The real part of the two oriented transfer functions with $k_{nc} = 0.5$ for clockwise and counterclockwise spindle rotation are shown in Fig. 3(b). The limiting chip width b_c is determined by the negative real part σ_r of the oriented transfer function according to Eq. (13). Especially for the structural modes with low frequencies the oriented transfer functions are completely different for the two opposite orientations of the tangential cutting force. The chatter frequencies are shown in Fig. 3(c). For clockwise spindle rotation they are mainly between 75 Hz and 125 Hz, which correspond to the minima of the real part σ_r of the oriented transfer function (cf. Fig. 3(b)). For counterclockwise rotation chatter frequencies or negative minima of σ_r, respectively, can be found slightly larger than 75 Hz, 140 Hz and 1575 Hz. In Fig. 3(d) the stability lobes for the turning example for both rotational directions with a tangential cutting force coefficient $K_{tc} = 1500$ N/mm^2 are shown. They were calculated directly from the measured frequency response data. The structure of the stability lobes is completely different for the two rotational directions and there is roughly a factor two between the global minima of the lobes. Hence, the cross FRF has a significant influence on the chatter vibrations in turning and causes a different location of the stability lobes and different chatter frequencies for different rotational directions of the spindle.

In some situations the cross FRF can also dominate the oriented transfer function. This situation occurs for the mode with an eigenfrequency of 140 Hz and is emphasized by dotted circles in Fig. 3. For this structural mode the magnitude of the cross FRF is approximately equal to the magnitude of the direct FRF as can be seen in Fig. 3(a). The behavior of the real part σ_r of the oriented transfer function is domi-

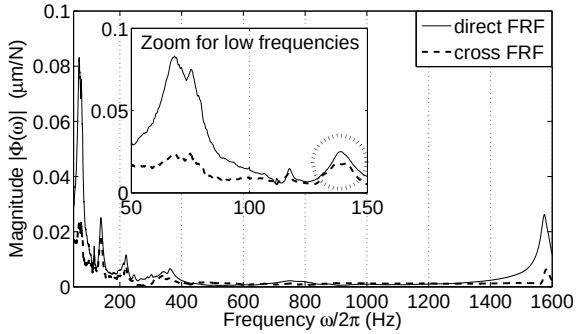

(a) Magnitude of direct Φ_{yy} (solid) and cross FRF Φ_{yx} (dashed) at the tool tip of a real lathe.

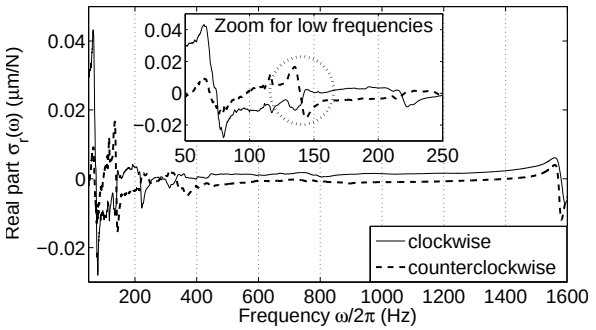

(b) Real part $\sigma_r(\omega)$ of the oriented transfer function for turning with clockwise (solid) and counterclockwise (dashed) spindle rotation.

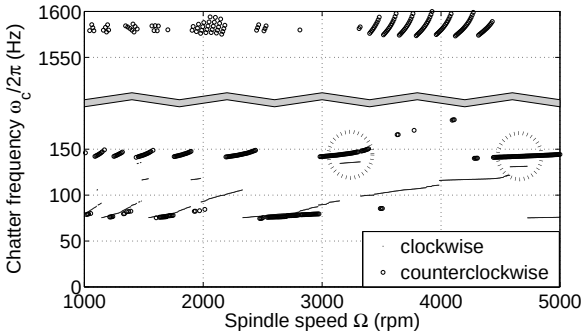

(c) Chatter frequencies ω_c for turning with clockwise (solid) and counterclockwise (circles) spindle rotation.

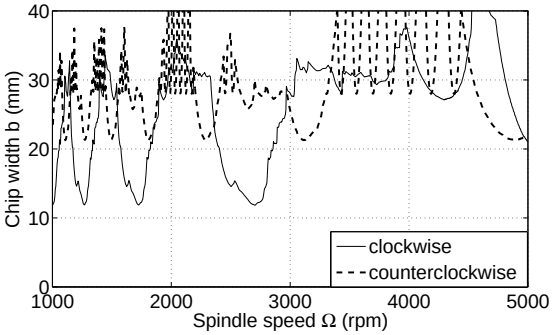

(d) Critical chip width b_c for turning with clockwise (solid) and counterclockwise (dashed) spindle rotation.

Figure 3: The magnitude of the cross FRF Φ_{yx} is smaller than the magnitude of the direct FRF Φ_{yy} (a), but the cross FRF is responsible for the significantly different behavior of the oriented transfer functions (b), chatter frequencies (c) and stability lobes (d) for the two different rotational directions.

nated by the cross FRF Φ_{yx}. For frequencies around the eigenfrequency of 140 Hz, according to Eq. (22) the sign of σ_r is opposite for the two opposite rotational directions (see Fig. 3(b)). Consequently, the local minima of σ_r and the chatter frequencies ω_c are lower than 140 Hz for clockwise rotation and larger than 140 Hz for counterclockwise rotation. This can be seen in Fig 3(c) at 3200 rpm and 4600 rpm, where the limiting chip width b_c is determined by the 140 Hz mode. The case with lower eigenfrequencies for clockwise rotation is equivalent to the unusual case of a negative directional factor in the modal description of regenerative chatter in turning, where an increase of the cutting force tends to move the tool deeper into the workpiece [23].

The presented results for the dependence of the chatter stability on the rotational direction in turning are qualitatively independent of the cutting force behavior or the machine tool. A lower value of k_{nc} enhances the influence of the cross FRF on the stability and the differences between the lobes of clockwise and counterclockwise rotation are increased. Higher k_{nc} weakens the differences in the stability lobes of the two orientations.

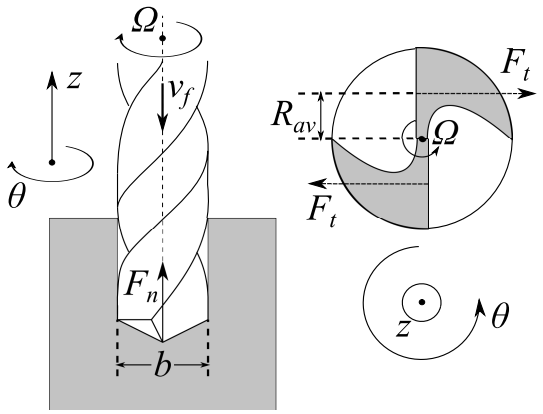

Figure 4: Geometry of a drilling process

4.3. Axial-torsional chatter in drilling

Under reasonable assumptions axial-torsional and lateral chatter in drilling is decoupled from each other and can be analyzed separately [22]. In [24] a model for axial-torsional chatter in drilling was introduced using modal coordinates of the drill. Here an alternative view on axial-torsional chatter vibrations in drilling is presented, where no modal analysis of the structure is required.

The geometry of a drilling process is illustrated in Fig. 4. Only the axial displacement z and the torsion angle θ of the tool are considered, $\mathbf{r} = (z, \theta)^T$. The normal direction $\mathbf{e}_h$ and the matrix $\mathbf{T}$ for this process are

$$\mathbf{e}_h = \begin{pmatrix} 1 \\ 0 \end{pmatrix}, \quad \mathbf{T} = \begin{pmatrix} 0 & 1 \\ -R_{av} & 0 \end{pmatrix}, \tag{23}$$

Here, the matrix $\mathbf{T}$ transforms tangential F_t and normal cutting forces F_n at the cutting lips into axial forces F_z and moments M about the drill axis. In practice the moment M is generated by a force distribution along the cutting edge. In the theory the moment M is generated by the product of R_{av} with the tangential cutting force F_t, interpreted as a point force as illustrated in Fig. 4, which defines the radius R_{av}. The matrix of the structural FRFs and the coefficient matrix of the cutting force are

$$\mathbf{\Phi} = \begin{pmatrix} \Phi_{zz} & \Phi_{z\theta} \\ \Phi_{\theta z} & \Phi_{\theta\theta} \end{pmatrix}, \quad \mathbf{B}_c = \begin{pmatrix} k_{nc} & 0 \\ -R_{av} & 0 \end{pmatrix}. \tag{24}$$

The matrix $\mathbf{\Phi}$ specifies the structural behavior of axial-torsional vibrations at the tool tip. In particular Φ_{zz} and $\Phi_{z\theta}$ describe the behavior of axial displacements z in response to an axial force and a moment, respectively. The behavior of torsional displacements θ in response to an axial force and a moment is characterized by the FRFs $\Phi_{\theta z}$ and $\Phi_{\theta\theta}$, respectively. Again for convenience no process damping is considered but could be easily included. According to Eq. (12b) the nonzero eigenvalue of the matrix product $\mathbf{\Phi}\mathbf{B}_c$ determines the oriented transfer function

$$\sigma(\omega) = \Phi_{zz}(\omega) k_{nc} - \Phi_{z\theta}(\omega) R_{av}. \tag{25}$$

Bayly et al. [24] have shown that the structural behavior of a twist drill is comparable to the behavior of a twist beam. The cutting torque against the rotational direction untwists the drilling tool. This is associated with an increase in its length. In other words, the axial cutting force leads to a decrease of the drill length, whereas simultaneously the tangential cutting force tends to increase the length. In [24] the structural dynamics in axial direction is dominated by the cross FRF $\Phi_{z\theta}$ or the structural displacements in response to a torque, respectively. This leads to a negative directional factor in the modal description and chatter frequencies below the eigenfrequency of the critical axial-torsional mode.

An optimal balance between the two mechanisms of increasing and decreasing drill length due to normal and tangential cutting forces is characterized by a cancellation of the two terms in Eq. (25) resulting in $\sigma = 0$. Theoretically, in this case axial-torsional chatter vibrations are completely eliminated. In practice at least a stabilization of axial-torsional vibrations in drilling is possible by raising the negative minimum of the real part σ_r of the oriented transfer function. Thus, Eq. (25) is suitable for an optimization of the structural behavior during the design of drilling tools.

4.4. Slot milling

In general a milling cutter has multiple teeth resulting in more than one matrix $\mathbf{T}$ and multiple cuts with normal directions $\mathbf{e}_h$. Furthermore, the process geometry is time-varying due to the rotation of the cutter, $\mathbf{T} = \mathbf{T}(t)$ and $\mathbf{e}_h = \mathbf{e}_h(t)$. The analysis in

Appendix A or the formulas in [3, 4, 20] can be used for the calculation of the coefficient matrix $\mathbf{B}_c$. In the case of slot milling with full radial immersion of a uniform tool with four teeth and negligible process damping one obtains

$$\mathbf{B}_c = \begin{pmatrix} k_{nc} & +1 \\ -1 & k_{nc} \end{pmatrix}. \tag{26}$$

Indeed, the matrix of directional factors in Eq. (26) is time-averaged but for full immersion milling this zeroth-order approximation leads only to slightly different stability lobes in comparison to the lobes with exact time-variant cutting force coefficients [3, 4, 16, 20]. If cross FRFs of the structure can be dropped the two eigenvalues of the matrix product $\mathbf{\Phi B}_c$ are

$$\sigma_{1,2}(\omega) = k_{nc}\frac{\Phi_{xx}(\omega)+\Phi_{yy}(\omega)}{2} \pm \sqrt{\frac{k_{nc}^2}{4}(\Phi_{xx}(\omega)-\Phi_{yy}(\omega))^2 - \Phi_{xx}(\omega)\Phi_{yy}(\omega)}. \tag{27}$$

In contrast to the previous one dimensional examples, the two generalized oriented transfer functions for slot milling $\sigma_{1,2}(\omega)$ of Eq. (27) cannot be written as a superposition similar to Eq. (14). In fact, they are the exact oriented transfer functions and include the two-dimensional coupled dynamics during the process at the stability border. The $\sigma_{1,2}(\omega)$ in Eq. (27) can be used for computing the stability lobes with our generalization of Tlusty's law, Eq. (13). In addition they are suited for getting insight into the chatter mechanism in milling. Two limiting cases are investigated in the following.

The first case corresponds to a structural behavior which is dominated by a single mode. If the direct FRF in mode direction is characterized by Φ_m and there is an angle α between the mode orientation and the feed direction x, the matrix with the FRFs in Cartesian coordinates can be written as

$$\mathbf{\Phi}(\omega) = \Phi_m(\omega)\begin{pmatrix} \cos(\alpha)^2 & \sin(\alpha)\cos(\alpha) \\ \cos(\alpha)\sin(\alpha) & \sin(\alpha)^2 \end{pmatrix}. \tag{28}$$

Obviously, in this limiting case the problem drops down to a scalar problem. There is only one nonzero eigenvalue of the eigenvalue problem of Eq. (12b) with the eigenvector $\mathbf{v} = (\cos(\alpha), \sin(\alpha))^T$. This corresponds to a tool vibration in the mode direction. The nonzero eigenvalue $\sigma = k_{nc}\Phi_m$ is independent of the mode orientation α. It can be interpreted as the oriented transfer function for this one-dimensional approximation of the milling process dynamics. The special case with $\alpha = 90°$ coincides with an example shown in [3].

The second case is the limiting case of a symmetric structural behavior, where the FRFs in $x-$ and $y-$ direction are equal, $\Phi_{xx} = \Phi_{yy} = \bar{\Phi}$. In this case the two generalized oriented transfer functions of Eq. (27) are $\sigma_{1,2}(\omega) = \bar{\Phi}(\omega)(k_{nc} \pm i)$. According to Eq. (13) the negative real part of $\sigma(\omega)$ determines positive critical chip widths b_c. Thus, as long as the imaginary part $\bar{\Phi}_i$ of the FRF is negative, only the eigenvalue

$$\sigma(\omega) = \bar{\Phi}(\omega)(k_{nc} - i), \quad \text{with} \tag{29a}$$
$$\sigma_r(\omega) = \bar{\Phi}_r(\omega)k_{nc} + \bar{\Phi}_i(\omega), \tag{29b}$$

is relevant for the calculation of stability lobes for slot milling with a nearly symmetric tool. Moreover, for typical structural and process parameters k_{nc} can be assumed to be zero in Eq. (29a) and Eq. (29b) resulting in

$$\sigma(\omega) \approx -i\bar{\Phi}(\omega), \quad \text{with} \tag{30a}$$
$$\sigma_r(\omega) \approx \bar{\Phi}_i(\omega). \tag{30b}$$

The corresponding eigenvector is $\mathbf{v} = (i, 1)^T$, which means a circular tool vibration in the x-y-plane. Even though, there is a strong coupling between the two spatial directions and the chatter problem is obviously two-dimensional, the stability behavior can be obtained from Eq. (13). However, in the approximation of Eq. (30b) the imaginary part of the FRF determines the real part σ_r of the generalized oriented transfer function and the limiting chip width b_c. This is opposite to turning, drilling and other one-dimensional processes where the real part of the FRFs determines the limiting chip width. As a consequence the chatter frequencies at the stability lobes in milling are not strictly below or above the critical eigenfrequencies of the structure but rather around the eigenfrequencies of the structure.

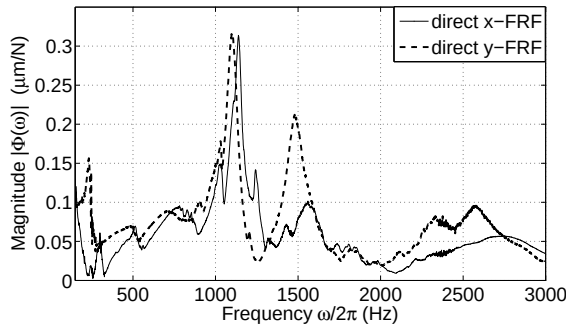

(a) Magnitude of direct FRFs Φ_{xx} (solid) and Φ_{yy} (dashed) in the lateral x- and y-direction at the tool tip of an end mill.

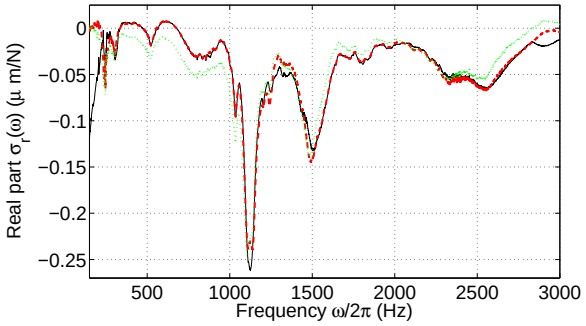

(b) Real part σ_r of the exact (solid, black) oriented transfer function Eq. (27) and approximations Eq. (29b) (dashed, red) and Eq. (30b) (dotted, green).

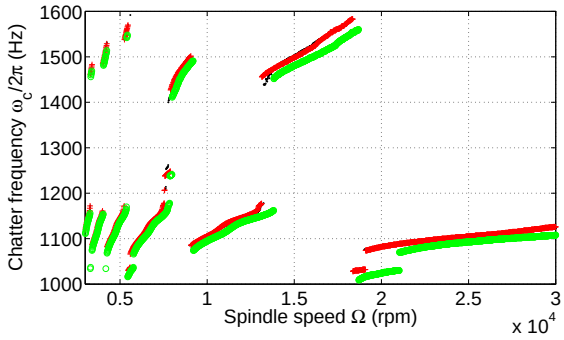

(c) Chatter frequencies ω_c for exact (black dots) $\sigma(\omega)$ Eq. (27) and for approximations Eq. (29b) (red crosses) and Eq. (30b) (green circles).

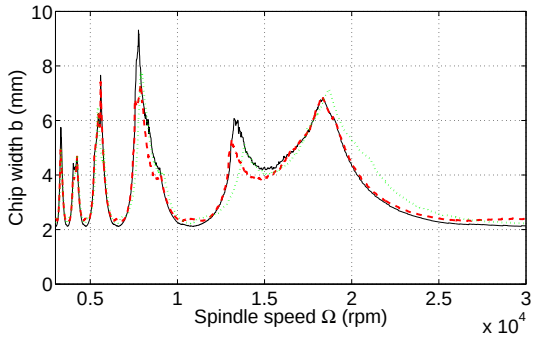

(d) Critical chip width b_c for exact (solid, black) $\sigma(\omega)$ Eq. (27) and approximations of Eq. (29b) (dashed, red) and Eq. (30b) (dotted, green).

Figure 5: (Color online). The magnitude of the direct FRFs Φ_{xx}, Φ_{yy} in x-, y-direction are approximately equal (a) and the exact oriented transfer function of Eq. (27) can be approximated by Eq. (29b) and Eq. (30b) (b). As a result there are nearly no differences between the exact and the approximated chatter frequencies (c) and stability lobes (d).

Especially the approximation for symmetric structural behavior seems to be relevant in a wide range of cutting conditions and applications. In Fig. 5 the accuracy of the approximations Eq. (29b) and Eq. (30b) for the generalized oriented transfer functions is demonstrated for experimental data of a real slot milling process. In Fig. 5(a) experimental measurements of direct FRFs in x- and y-direction of a milling cutter at the tool tip are shown. The end mill with a diameter of 20 mm and a length of 104 mm was mounted in a Starrag Heckert HEC 500 machining center. The dominant eigenfrequencies of the tool in x- and y-direction are close to each other at 1100 and 1140 Hz. In y-direction also a peak at 1475 Hz occurs. The exact real part of the relevant generalized oriented transfer function according to Eq. (27) as well as the proposed approximations Eq. (29b) and Eq. (30b) are shown in Fig. 5(b). Since in this practical example the direct FRFs Φ_{xx} and Φ_{yy} in $x-$ and $y-$ direction do not match exactly, the relation $\bar{\Phi} = (\Phi_{xx} + \Phi_{yy})/2$ is used for the approximations. The ratio between normal and tangential shearing force is set to $k_{nc} = 0.3$. Both approximations fit the exact eigenvalue very well especially around the

negative minimum of the real part. The chatter frequencies are shown in Fig. 5(c). As expected from the theory and contrary to the turning example they are not merely below or above the eigenfrequencies of the structure at 1100 Hz, 1140 Hz and 1475 Hz but rather around them. In Fig. 5(d) the stability lobes are presented for a tangential cutting force coefficient $K_{tc} = 900$ N/mm^2. It can be seen that the difference between exact and approximated stability lobes is very small. Already the simple approximation with the averaged imaginary part $\bar{\Phi}_i$ (dotted, green) of the FRF according to Eq. (30b) is sufficient for the identification of the stability lobes for full-immersion slotting. It can be used for an optimization of the structure of machine tools and for an optimization of the cutting process.

5. Conclusion

A unified approach for the stability analysis of regenerative chatter in machining is presented. The analysis in the frequency domain can be used for the calculation of stability lobes for turning, drilling, boring or milling by taking into account process damping. The procedure is quite simple and can be used for the identification of stability lobes in a few seconds without the necessity of any iteration. Because no modal analysis is necessary the method is suitable for an implementation directly on the numerical control of a machine tool.

Furthermore, a unified treatment of the eigenvalue problem for the determination of the stability lobes in the absence of process damping is presented based on a generalization of the well-known stability law of Tlusty in Eq. (13). It is shown, that the eigenvalues of the product of the matrices of the FRFs and the directional factors are generalized oriented transfer functions in multi-dimensional cutting processes. Oriented transfer functions are derived for basic turning and drilling examples. They give an alternative insight into the dependence of the stability lobes on the rotational direction in turning and on the axial-torsional structural coupling in drilling. For the coupled two-dimensional dynamics in slot milling the generalized oriented transfer functions are derived.

In particular for slot milling with a nearly symmetric structural behavior it was revealed and verified by experimental data, that in fact the limiting chip width is determined by the imaginary part rather than the real part of the structural FRF. The presented approximations of the relevant generalized oriented transfer function for milling still contain the coupled two-dimensional dynamics and they are not comparable to existing one-dimensional approximations of the milling process. The resulting simple relation between structural FRF and the limiting chip width can be used for an efficient optimization of machine tool structures with respect to dynamic stability already during the design stage.

Acknowledgment

This work was partially supported by the research and development project ReffiZ, which was funded by the German Federal Ministry of Education and Research (BMBF) within the Framework Concept "Research for Tomorrow's Production" (fund number 02PC1010) and managed by the Project Management Agency Forschungszentrum Karlsruhe (PTKA). We would like to thank Dr. Josef Kleckner for helpful discussions.

Appendix A. Cutting force model for complex process geometry

In this section a detailed description for the determination of the cutting force coefficient matrices $\mathbf{B}_c$ and $\mathbf{B}_d$ is given. It is applicable for complex process geometries with multiple cuts and time-variant orientations, as well as for considering nonlinear cutting force laws and forces into a third spatial direction.

Appendix A.1. Cutting force law

The cutting force law describes the differential cutting force

$$d\mathbf{F}_{tna}(t, \mathbf{\Delta}, \dot{\mathbf{r}}; i, z) = \left(\mathbf{f}_c(h(t, \mathbf{\Delta}; i, z)) + \mathbf{K}_d \mathbf{e}_h^T \tau \dot{\mathbf{r}}\right) dz \tag{A.1}$$

in local tangential, normal and axial coordinates at the cutting edge for differenatial segments dz of the

chip width. The function $\mathbf{f}_c(h)$ specifies the possibly nonlinear behavior of the shear forces and the vector $\mathbf{K}_d =$ the behavior of the process damping force. Some empirical laws for the shear force are summarized in [9] and some laws for the process damping force can be found in [5, 6, 7].

Appendix A.2. Chip thickness

The chip thickness at the ith cutting tooth and position z

$$h = h(t, \mathbf{\Delta}; i, z) \tag{A.2}$$

is a function of time t and of regenerative dynamic displacements $\mathbf{\Delta}$ of the tool center point

$$\mathbf{\Delta}(t) = \mathbf{r}(t - \tau) - \mathbf{r}(t). \tag{A.3}$$

The explicit form of the chip thickness h depends on the specific geometry of the process.

Appendix A.3. Process force

The differenatial cutting forces $d\mathbf{F}_{tna}$ in local coordinates at the cutting edges are transformed via the 4×3 matrix $\mathbf{T}(t; i, z)$ into differntial cutting forces in Cartesian coordinates

$$d\mathbf{F}(t, \mathbf{\Delta}, \dot{\mathbf{r}}; i, z) = \mathbf{T}(t; i, z) d\mathbf{F}_{tna}(t, \mathbf{\Delta}, \dot{\mathbf{r}}; i, z). \tag{A.4}$$

The process force is the summation of the differential components $d\mathbf{F}$ over all N teeth integrated from $z = 0$ to the chip width b

$$\mathbf{F}(t, \mathbf{\Delta}, \dot{\mathbf{r}}) = \sum_{i=1}^{N} \int_0^b d\mathbf{F}(t, \mathbf{\Delta}, \dot{\mathbf{r}}; i, z). \tag{A.5}$$

It can be separated into shear forces and process damping forces as

$$\mathbf{F}(t, \mathbf{\Delta}, \dot{\mathbf{r}}) = \mathbf{F}_c(t, \mathbf{\Delta}) + \mathbf{F}_d(\dot{\mathbf{r}}) \tag{A.6a}$$

$$\mathbf{F}_c(t, \mathbf{\Delta}) = \sum_{i=1}^{N} \int_0^b \mathbf{T}(t; i, z) \mathbf{f}_c(h(t, \mathbf{\Delta}; i, z)) dz \tag{A.6b}$$

$$\mathbf{F}_d(\dot{\mathbf{r}}) = \sum_{i=1}^{N} \int_0^b \mathbf{T}(t; i, z) \mathbf{K}_d \mathbf{e}_h^T \tau \dot{\mathbf{r}}(t) dz \tag{A.6c}$$

$$\mathbf{F}_d(\dot{\mathbf{r}}) = -bK_{tc} \mathbf{B}_d(t) \tau \dot{\mathbf{r}}(t), \tag{A.6d}$$

where Eq. (A.6d) is the expression of the process damping force similar to Eq. (4). By comparing Eq. (A.6c) and Eq. (A.6d) the coefficient matrix of the process damping force can be identified as

$$\mathbf{B}_d(t) = -\frac{1}{b\tau K_{tc}} \sum_{i=1}^{N} \int_0^b \mathbf{T}(t; i, z) \mathbf{K}_d \mathbf{e}_h^T dz. \tag{A.7}$$

Appendix A.4. Linearization

Typically the process force $\mathbf{F}(t, \mathbf{\Delta}, \dot{\mathbf{r}})$ depends nonlinearly on the regenerative displacements $\mathbf{\Delta}$. The chatter instability is determined by the exponential behavior of small dynamic perturbations $\mathbf{r}_{\text{dyn}}$ of the stable cutting dynamics. Stable cutting is typically characterized by a periodic relative motion $\mathbf{r}_s$ between tool and workpiece with the spindle rotation period and with $\mathbf{\Delta} = \mathbf{0}$. The dynamics of the perturbed solution $\mathbf{r} = \mathbf{r}_s + \mathbf{r}_{\text{dyn}}$ is composed of the solution for stable cutting $\mathbf{r}_s$ and the small perturbation $\mathbf{r}_{\text{dyn}}$. The dynamic process force $\mathbf{F}_{\text{dyn}}$, which describes the difference of the force between the perturbed and the stable solution, is obtained by linearization of the process force $\mathbf{F}(t, \mathbf{\Delta}, \dot{\mathbf{r}})$ of Eq. (A.6a) around $\mathbf{\Delta} = \mathbf{0}$

$$\begin{aligned} \mathbf{F}_{\text{dyn}}(t, \mathbf{\Delta}, \dot{\mathbf{r}}) = {} & \left. \frac{d\mathbf{F}_c(t, \mathbf{\Delta})}{d\mathbf{\Delta}} \right|_{\mathbf{\Delta}=\mathbf{0}} \mathbf{\Delta}_{\text{dyn}}(t) \\ & - bK_{tc} \mathbf{B}_d(t) \tau \dot{\mathbf{r}}_{\text{dyn}}(t), \end{aligned} \tag{A.8}$$

where $\frac{d\mathbf{F}_c}{d\mathbf{\Delta}}$ denotes the Jacobian of $\mathbf{F}_c(t, \mathbf{\Delta})$ of Eq. (A.6a). By comparison of Eq. (A.6a) and Eq. (4) the coefficient matrix of the dynamic shear force can be determined by

$$\mathbf{B}_c(t) = \frac{1}{bK_{tc}} \sum_{i=1}^{N} \int_0^b \mathbf{T}(t; i, z) \mathbf{f}_c'(h(t, \mathbf{0}; i, z)) \frac{dh}{d\mathbf{\Delta}} dz, \tag{A.9}$$

with the derivative $\mathbf{f}_c'$ of the cutting force law.

Appendix A.5. Zeroth order approximation

For a complex process geometry the cutting force coefficients are time variant with period T of the spindle rotation as can be seen from Eq. (A.7) and Eq. (A.9). For the chatter stability analysis in many

cases the zeroth order approximation is sufficient, which takes only the zeroth component of the Fourier series into account. Then the coefficient matrices for the dynamic process force are just the time averages over one period

$$\bar{\mathbf{B}}_c = \frac{1}{T}\int_0^T \mathbf{B}_c(t)dt, \quad \bar{\mathbf{B}}_d = \frac{1}{T}\int_0^T \mathbf{B}_d(t)dt. \quad \text{(A.10)}$$

The averaged coefficient matrices $\bar{\mathbf{B}}_c$ and $\bar{\mathbf{B}}_d$ can be used for the frequency domain stability analysis in Sec. 3.

References

[1] O. Danek, M. Polacek, J. Spacek, J. Tlusty, Selbsterregte Schwingungen an Werkzeugmaschinen, VEB Technik Berlin, Berlin, 1962.

[2] S. A. Tobias, Schwingungen an Werkzeugmaschinen, Hanser, München, 1961.

[3] Y. Altintas, M. Weck, Chatter Stability of Metal Cutting and Grinding, CIRP Annals 53 (2004) 619 – 642.

[4] Y. Altintas, Manufacturing Automation: Metal Cutting Mechanics, Machine Tool Vibrations, and CNC Design, Cambridge University Press, 2012.

[5] Y. Altintas, M. Eynian, H. Onozuka, Identification of dynamic cutting force coefficients and chatter stability with process damping, CIRP Annals - Manufacturing Technology 57 (1) (2008) 371 – 374.

[6] E. Budak, L. Tunc, Identification and modeling of process damping in turning and milling using a new approach, CIRP Annals - Manufacturing Technology 59 (1) (2010) 403 – 408.

[7] V. Sellmeier, B. Denkena, High speed process damping in milling, CIRP Journal of Manufacturing Science and Technology 5 (1) (2012) 8 – 19.

[8] C. Tyler, T. Schmitz, Analytical process damping stability prediction, Journal of Manufacturing Processes 15 (1) (2013) 69 – 76.

[9] G. Stepan, Z. Dombovari, J. Muñoa, Identification of cutting force characteristics based on chatter experiments, CIRP Annals - Manufacturing Technology 60 (1) (2011) 113 – 116.

[10] M. Zatarain, I. Bediaga, J. Muñoa, R. Lizarralde, Stability of milling processes with continuous spindle speed variation: Analysis in the frequency and time domains, and experimental correlation, CIRP Annals - Manuf. Techn. 57 (1) (2008) 379 – 384.

[11] A. Otto, G. Kehl, M. Mayer, G. Radons, Stability Analysis of Machining with Spindle Speed Variation, Adv. Mater. Res. 223 (2011) 600 – 609.

[12] D. Bachrathy, G. Stepan, J. Turi, State Dependent Regenerative Effect in Milling Processes, Journal of Computational and Nonlinear Dynamics 6 (4) (2011) 041002.

[13] A. Otto, G. Radons, Application of spindle speed variation for chatter suppression in turning, CIRP Journal of Manufacturing Science and Technology 6 (2) (2013) 102 – 109.

[14] A. Otto, G. Radons, The influence of tangential and torsional vibrations on chatter stability lobes, submitted, (2014).

[15] Z. Dombovari, Y. Altintas, G. Stépán, The effect of serration on mechanics and stability of milling cutters, Int. J. Mach. Tools Manuf. 50 (2010) 511 – 520.

[16] V. Sellmeier, B. Denkena, Stable islands in the stability chart of milling processes due to unequal tooth pitch, Int. J. Mach. Tools Manuf. 51 (2011) 152 – 164.

[17] A. Otto, G. Radons, Frequency domain stability analysis of milling processes with variable helix tools, 9th Int. Conf. on High Speed Machining, San Sebastian, Spain, March 7-8 .

[18] J. Zulaika, F. Campa, L. L. de Lacalle, An integrated process–machine approach for designing productive and lightweight milling machines, International Journal of Machine Tools and Manufacture 51 (7–8) (2011) 591 – 604.

[19] P. Albertelli, N. Cau, G. Bianchi, M. Monno, The effects of dynamic interaction between machine tool subsystems on cutting process stability, The International Journal of Advanced Manufacturing Technology 58 (9-12) (2012) 923–932.

[20] Y. Altintas, E. Budak, Analytical Prediction of Stability Lobes in Milling, CIRP Annals - Manuf. Techn. 44 (1) (1995) 357 – 362.

[21] Y. Altintas, Z. Kilic, Generalized dynamic model of metal cutting operations, CIRP Annals - Manufacturing Technology 62 (1) (2013) 47 – 50.

[22] J. Roukema, Y. Altintas, Generalized modeling of drilling vibrations. Part II: Chatter stability in frequency domain, Int. J Mach. Tools Manuf. 47 (9) (2007) 1474 – 1485.

[23] M. Zatarain, I. Bediaga, J. Muñoa, T. Insperger, Analysis of directional factors in milling: importance of multi-frequency calculation and of the inclusion of the effect of the helix angle, Int. J. Adv. Manuf. Techn. 47 (2010) 535 – 542.

[24] P. Bayly, S. Metzler, A. Schaut, K. Young, Theory of Torsional Chatter in Twist Drills: Model, Stability Analysis and Composition to Test., J. Manuf. Sci. Eng. 123 (4) (2002) 552–561.